Anion directed cation templated synthesis of three ternary copper(II) complexes with a monocondensed N_2O donor Schiff base and different pseudohalides

Prasanta Bhowmik[a], Anik Bhattacharyya[a], Klaus Harms[b], Stephen Sproules[c], Shouvik Chattopadhyay[a,*]

[a] *Department of Chemistry, Inorganic Section, Jadavpur University, Kolkata -700 032, India.*

e-mail: shouvik.chem@gmail.com Tel:+(91)33-2457-2941

[b] *Fachbereich Chemie, Philipps-Universität Marburg, Hans-Meerwein-Straße, 35032 Marburg, Germany.*

[c] *WestCHEM, School of Chemistry, University of Glasgow, Glasgow G12 8QQ, United Kingdom.*

Abstract

Three copper(II) complexes, $[Cu_2(L)_2(\mu_{1,1}\text{-}N_3)_2]$ **(1)**, $[Cu_2(L)_2(\mu_{1,1}\text{-}NCO)_2]$ **(2)** and $[Cu(L)(\mu_{1,5}\text{-}dca)]_n$ **(3)**, where *HL* is a tridentate mono-condensed Schiff base, 1-(2-aminoethyliminomethyl)naphthalen-2-ol, and dca is dicyanamide, have been prepared and characterized by elemental analysis, IR, UV–Vis and fluorescence spectroscopy and single crystal X-ray diffraction studies. The Schiff base ligand is prepared by counter anion mediated copper(II) templated synthesis. Azide in complex **1** and cyanate in complex **2** show μ-1,1 bridging modes; whereas dca shows μ-1,5 bridging mode in complex **3**. Three equatorial

positions of copper(II) are occupied by the tridentate Schiff bases in all the three complexes. The fourth equatorial sites are occupied by nitrogen atoms of azide in **1**, cyanate in **2** and dca in **3**. Another nitrogen atom from a symmetry related pseudohalide coordinates the axial position of copper(II) to complete its square pyramidal geometry in each of the complexes. Significant supramolecular interactions are observed in all the complexes. Variable temperature magnetic measurements indicate antiferromagnetic interactions between copper(II) centres in all the three complexes.

Key words: Copper(II); Schiff base; pseudo halide; template synthesis; antiferromagnetic.

1. Introduction

The 1:1 condensation of diamines with salicyaldehyde or its derivatives may produce 'half salen' type ligands. Elder reported a very convenient template synthesis of the nickel(II) complex for the half unit of salicylaldehyde with various diamines [1]. The ligand could be freed by precipitating nickel(II) as a DMG complex [2]. The ligands could then be used to form copper(II) complexes [3]. This method fails to prepare the mono-condensed Schiff base from 1,2-diaminoethane and salicylaldehyde derivatives [4]. Copper(II) complexes of such ligands could therefore be obtained with the help of the copper(II) template effect [5-10]. In this method, the copper(II) is first made to react with the salicylaldehyde or its derivatives. Then a suitable coordinating anion is added, followed by the addition of the diamime. In the present work, we have applied the same methodology to prepare a mono-condensed N_2O donor tridentate Schiff base, *HL* (1-(2-aminoethyliminomethyl)naphthalen-2-ol) using 1,2-diaminoethane and 2-hydroxynaphthaldehyde (Scheme 1).

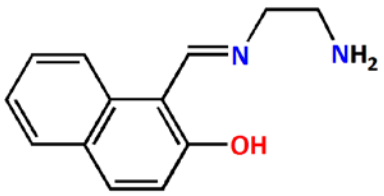

HL

Scheme 1: Molecular structure of the ligand, HL, used in the work.

The rational design and synthesis of di and polynuclear transition metal complexes are of immense importance now-a-days, because of their diverse structures [11-15] and magnetic properties [16-20]. Pseudohalides, especially azide, cyanate and thiocyanate, have widely been employed for the syntheses of such systems because of their ability to coordinate metal ions with different modes [21-23]. Dicyanamide is sometimes called bent pseudohalide [24-25] and the coordination polymers based on dicyanamide (dca) have also attracted much attention in the past few years for their interesting extended architectures and magnetic properties as well [26-. 30]. The pseudohalides may bind the adjacent metal centres in basal–basal (symmetric) [31] and basal–apical (unsymmetric or antisymmetric) modes [32-33] Regarding the basal–basal bridging mode of end-on pseudo-halides, the nature of the exchange coupling changes from ferromagnetic to antiferromagnetic, when the Cu–N–Cu angle crosses a critical value of 108^0 [34-35] On the other hand, basal–apical bridges for end-on modes usually give rise to very small magnetic couplings and the Cu–N–Cu angle is not indicative of the magnetic interaction [36]. Instead, several other factors, such as the steric and electronic factors of the blocking ligand, Cu…Cu distance, axial and equatorial Cu–N bond distances, hydrogen bonding interactions, etc. play vital roles in determining the magnitude and sign of the coupling constants [36] and as a result, it is difficult to arrive at any clear-cut magneto-structural

correlation. Keeping this in mind, we planned to synthesize more such complexes using the same blocking ligand to have a better insight into the magnetic properties of these complexes.

In the present work, we have used three pseudohalides viz. azide, cyanate and dicyanamide to prepare two dinuclear and a polynuclear copper(II) complexes, $[Cu_2(L)_2(\mu_{1,1}\text{-}N_3)_2]$ **(1)**, $[Cu_2(L)_2(\mu_{1,1}\text{-}NCO)_2]$ **(2)** and $[Cu(L)(\mu_{1,5}\text{-}dca)]_n$ **(3)**, with a mono-condensed N_2O donor tridentate Schiff base (HL) by anion directed cation templated syntheses. Herein, we would like to report the synthesis, spectroscopic characterization, crystal structures, supramolecular assemblies and magnetic properties of the complexes.

2. Experimental Section

Materials

All starting materials were commercially available, reagent grade, and used as purchased from Sigma-Aldrich without further purification.

*2.1.1 Synthesis of $[Cu_2(L)_2(\mu_{1,1}\text{-}N_3)_2]$ (**1**)*

Copper(II) acetate monohydrate (0.2 g, 1 mmol) was added to a methanol solution (10 ml) of 2-hydroxy-1-naphthaldehyde (0.172g, 1 mmol) to produce a green coloured solution. A methanol-water mixture of sodium azide (0.065 g, 1mmol) was then added to the resulting solution and stirred for ca. 30 min. A methanol solution of 1, 2-diaminoethane was added slowly to the mixture with constant stirring. The mixture was then refluxed for ca. 45 min. Appearance of a small amount of precipitate was filtered off. A crystalline complex was obtained on slow evaporation of the reaction mixture in open atmosphere. X-ray diffraction quality, dark green, block shaped single crystals were obtained from DMF solution after ~ 10 days.

Yield: 0.465 g (73%); Anal. Calc. for $C_{26}H_{26}Cu_2N_{10}O_2$ (637.65): C, 48.97; H, 4.11; N, 21.97%. Found: C, 48.7; H, 4.2; N, 22.1 %. FT-IR (KBr, cm^{-1}): 3155, 3247 (ν_{NH2}), 2037 (ν_{N3}), 1623 ($\nu_{C=N}$); UV-Vis, λmax (nm) [$\varepsilon_{max}(dm^3mol^{-1}m^{-1})$] (acetonitrile): 382 ($2\times10^4$), 590 (257).

*2.1.2 Synthesis of [$Cu_2(L)_2(\mu_{1,1}$-NCO)$_2$] (**2**)*

It was prepared in a similar method as that of complex **1**, except that sodium cyanate (0.065 g, 1 mmol) was used instead of sodium azide. Single crystals, suitable for X-ray diffraction, were obtained from DMF solution after ~ 10 days.

Yield: 0.49 g (77%), Anal. Calc. for $C_{28}H_{26}Cu_2N_6O_4$ (637.63): C, 52.74; H, 4.11; N, 13.18 %. Found: C, 52.5; H, 4.2; N, 13.4 %. FT-IR (KBr, cm^{-1}): 3253, 3319 (ν_{NH2}), 2207 (ν_{NCO}), 1625 ($\nu_{C=N}$); UV-Vis, λ_{max} (nm) [$\varepsilon_{max}(dm^3mol^{-1}cm^{-1})$] (acetonitrile): 314 ($1.53\times10^4$), 393 ($1.01\times10^4$), 592 (133).

*2.1.3 Synthesis of [Cu(L)($\mu_{1,5}$-dca)]$_n$ (**3**)*

It was prepared in a similar method as that of complex **1**, except that sodium dicyanamide (0.09 g, 1 mmol) was used instead of sodium azide. X-ray diffraction quality single crystals were obtained after ~ 10 days on slow evaporation of the DMF solution of the complex in open atmosphere.

Yield: 0.24 g (71%), Anal. Calc. for $C_{15}H_{13}CuN_5O$ (342.84): C, 52.55; H, 3.82; N, 20.43 %. Found: C, 52.3; H, 3.6; N, 20.6 %. FT-IR (KBr, cm^{-1}): 3279, 3336 (ν_{NH2}), 2290, 2235, 2159 ($\nu_{N(CN)2}$), 1626 ($\nu_{C=N}$); UV-Vis, λ_{max} (nm) [$\varepsilon_{max}(dm^3\ mol^{-1}\ cm^{-1})$] (acetonitrile): 382 ($1.87\times10^4$), 593 (235).

2.2. Physical measurements

Elemental analysis (carbon, hydrogen and nitrogen) were performed using a PerkinElmer 240C elemental analyzer. IR spectra in KBr (4500–500 cm^{-1}) were recorded using a PerkinElmer Spectrum Two FT-IR Spectrometer. Electronic spectra in methanol (800–200 nm) were recorded in JASCO V-630 Spectrophotometer. Fluorescence spectra were obtained on Shimadzu RF-5301PC spectrofluorophotometer at room temperature. Magnetic data were recorded using a SQUID magnetometer (Quantum Design MPMS-XL) over a temperature range 2 – 300 K in a 1 T external field. Corrections for diamagnetism were made using Pascal's constants and magnetic data were corrected for diamagnetic contributions from the sample holder. Fits were performed using the program *JulX*.

2.3. X-ray Crystallography

Single crystals of the complexes of suitable dimensions were used for data collection using a Bruker D8 QUEST area detector diffractometer equipped with graphite-monochromated Mo-Kα radiation (λ= 0.71073 Å) at 100 K. The X-ray intensity data were measured. The frames were integrated with the Bruker SAINT software package using a wide-frame algorithm. The molecular structures were solved by direct method and refined by full-matrix least squares on F^2 using SHELXS-97 and SHELXL-2012 for complexes **1** and **3**; SHELXS-97 and SHELXL-2013 for complex **2** [37-38]. Non-hydrogen atoms were refined with anisotropic thermal parameters. The hydrogen atoms were placed in their geometrically idealized positions and constrained to ride on their parent atoms. Data were corrected for absorption effects using the multi-scan method (SADABS) [39]. Data collection software = BRUKER APEX II; Cell refinement software = SAINT V8.27B (Bruker AXS Inc., 2012); Data reduction software = SAINT V8.27B (Bruker AXS Inc., 2012). Significant crystallographic data are summarized in Table 1.

3. Result and Discussions

3.1 Synthesis

The formation of the complexes can be rationalized in the light of the templating effect of copper(II) modulated by the counter anions. The azide, cyanate or dca, having approximately similar crystal field stabilization energy as that of the Schiff bases, occupies one coordination site of copper(II), leaving the other three sites in the equatorial plane to be coordinated by the tridentate Schiff base and that can be achieved most efficiently by 'half-salen' type tridentate N_2O donor Schiff base ligands. In the present work, the 'half-salen' type mono-condensed Schiff base ligand, *HL*, was synthesized conveniently as the copper(II) complexes, $[Cu_2(L)_2(\mu_{1,1}\text{-}N_3)_2]$ (**1**), $[Cu_2(L)_2(\mu_{1,1}\text{-}NCO)_2]$ (**2**) and $[Cu(L)(\mu_{1,5}\text{-dca})]_n$ (**3**), by the reaction of 2-hydroxy-1-naphthaldehyde, copper(II) and sodium azide (for **1**) or sodium cyanate (for **2**) or sodium dicyanamide (for **3**) followed by the reaction with 1,2-diaminoethane. In the absence of the azide, cyanate or dca, a tetradentate Schiff base ligand is formed, produced by the 1:2 condensations of the 1,2-diaminoethane with 2-hydroxy-1-naphthaldehyde which, in turn, forms a square planar complex with copper(II), the structure of which was reported elsewhere [40]. Formations of all the complexes are shown in Scheme 2.

It may be noted here that the Schiff base ligand, *HL*, has previously been synthesized as a vanadium complex by a different group [41]. However, the synthesis and characterization of the free ligand by Elder's method [1], followed by the procedure used by Burke and McMillin [2] remained unsuccessful. The reason of this failure could be explained by the assumption of Ghosh et al [4]. According to Ghosh et al, formation of a tridentate mono-condensed Schiff base by Elder's method is possible only when it forms six or seven member chelate ring with nickel(II).

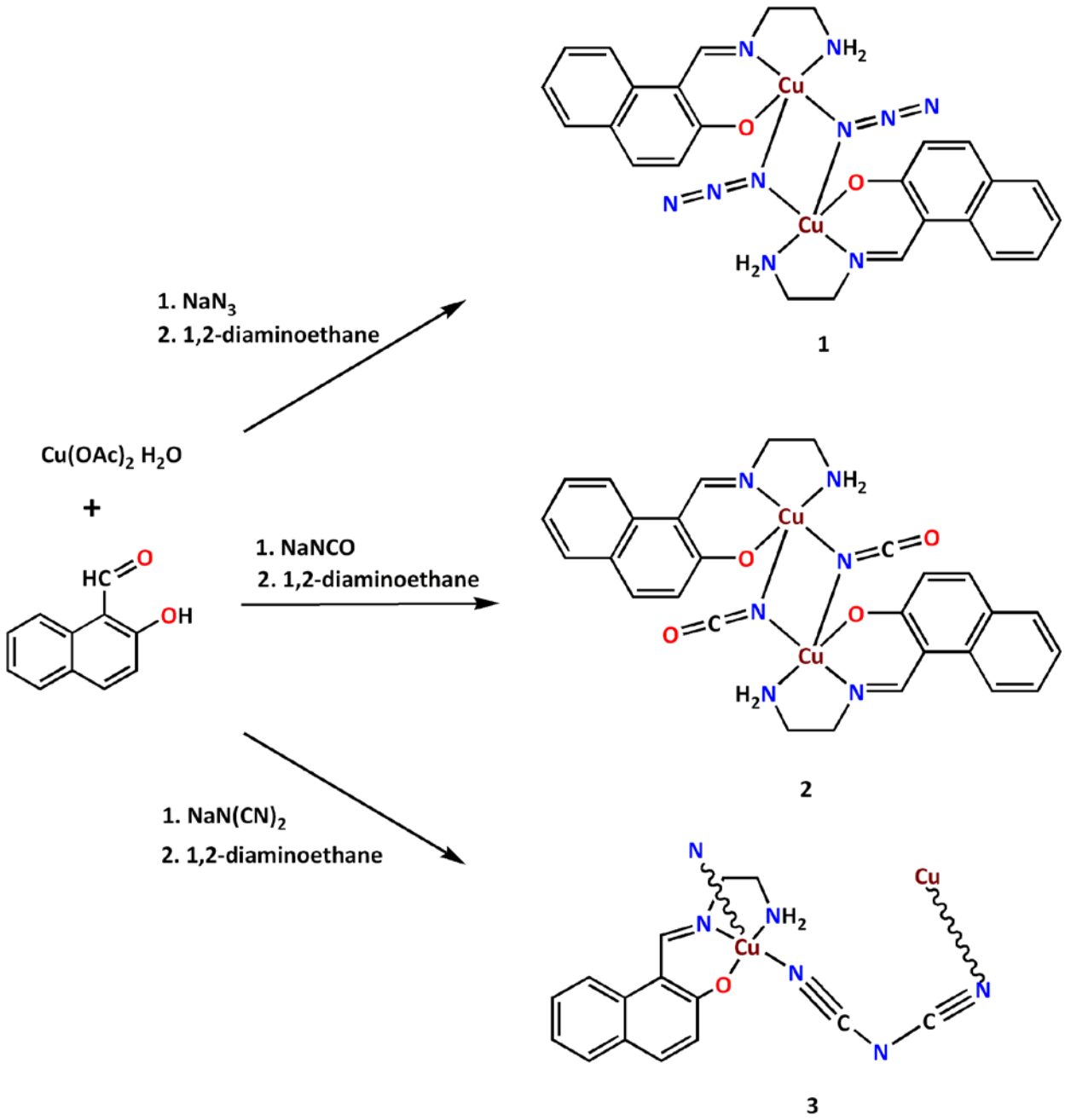

Scheme 2: Synthetic route of the complexes.

3.2 Description of the structures

*3.2.1 Complex $[Cu_2(L)_2(\mu_{1,1}\text{-}N_3)_2]$ (**1**) and $[Cu_2(L)_2(\mu_{1,1}\text{-}NCO)_2]$ (**2**)*

The structures of both **1** and **2** are centro-symmetric dimers in which the two copper(II) centres are five-coordinate being bonded to three donor atoms (N,N,O) of the deprotonated Schiff base (L^-) and two $\mu_{1,1}$ bridging anionic ligands, azide in **1** and cyanate in **2**.The geometry of a penta-coordinated metal complex may conveniently be measured by the Addison parameter [42], (trigonality index, $\tau = (\alpha\text{-}\beta)/60$, where α and β are the two largest L–M–L angles of the coordination sphere) that is ideally zero for a square-pyramidal complex and is one for a trigonal bi-pyramidal one. In both the complexes, copper(II) centres assume square pyramidal geometries with Addison parameters 0.17 in **1** and 0.05 in **2**. As usual for square pyramid structures, the copper(II) centres are slightly pulled out of the mean square planes towards the apical donor atoms at distances of 0.0933(3) Å in **1** and 0.0323(3) Å in **2**. The three donor atoms of the Schiff base occupy the equatorial plane while each of the two anionic ligands in the dimer occupy an equatorial position in one copper coordination sphere and an axial position at a longer distance in the other. The bond lengths in the equatorial plane are very similar in both the complexes. The copper(II)-oxygen distances lie in the range 1.906(2)-1.931(2) Å. The $Cu–N_{imine}$ distances are significantly shorter (1.937(2) Å for **1** and 1.932(2) Å for **2**) than the $Cu–N_{amine}$ distances (2.010(2) Å for **1** and 2.030(2) Å for **2**), as also observed in similar complexes [43-44]. The copper(II)-nitrogen(anion) bond lengths in the equatorial plane range from 1.951(2)-2.009(2) Å, while the copper(II)-nitrogen(anion) axial bond lengths range from 2.483(2)-2.528(2) Å.

Both the complexes **1** and **2** crystallize in monoclinic space group $P2_1/c$. The perspective views of **1** and **2** together with the atom numbering scheme are shown in Figures 1 and 2. The selected bond lengths and angles are gathered in Table 2. Deviations of the coordinating atoms,

N(1), N(4), O(1) and N(16) from the least-square basal planes are -0.186(2), 0.195(2), -0.187(2) and 0.178(2) Å respectively in **1** and are 0.084(2), -0.087(2), 0.082(2), and -0.080(2) Å respectively in **2** . The five membered chelate ring, Cu(1)–N(1)–C(2)–C(3)–N(4), assumes an intermediate conformation between half-chair and envelope being twisted on C(2)-C(3) with puckering parameters [45-47] Q(2) = 0.411(2) Å and ϕ(2) = 82.6(2)º in **1**. The same ring in **2** assumes envelope conformation with puckering parameters Q(2) = 0.407(2) Å and ϕ(2) =73.3(3)º. The bond lengths and angles are comparable with those for the related copper(II) complexes [36]. The bridging Cu_2N_2 network is perforce planar. The bridging pseudo-halides are quasi-linear with the N–N–N angle being 178.8(2)º in **1** and N–C–O angle being 177.5(3)º in **2**. The intra-dimer Cu···Cu distance is 3.158(1) Å in **1** and 3.1558(5) Å in **2**.

The hydrogen atoms, H(1A) and H(1B), attached to the nitrogen atom N(1) of complex **1** are involved in hydrogen bonding interactions with the symmetry related (^{a} = 1-x,1-y,1-z) phenoxo oxygen atom, $O(1)^a$ and azide nitrogen atom, $N(16)^d$ (^{d} = 2-x,1-y,1-z), respectively to form a one-dimensional chain along the crystallographic a axis, as shown in Figure 3. The hydrogen atom, H(1B), attached to the nitrogen atom, N(1) of complex **2** forms a hydrogen bond with a symmetry related (^{b} = -x,-y,1-z) phenoxo oxygen atom, $O(1)^b$, as shown in Figure 2. The details of hydrogen bonding interactions are gathered in Table 3.

Complex **1** shows significant C–H···π interactions. The hydrogen atom, H(2B), attached with C(2), is involved in one inter-molecular C–H···π interaction with a symmetry related (1-x,-1/2+y,1/2-z) phenyl ring, $\mathbf{R^5}$ [C(10)–C(11)–C(12)–C(13)–C(14)–C(15)]. Similarly, the hydrogen atom, H(3B), attached with C(3), is involved in another inter-molecular C–H···π interaction with a symmetry related (1-x,-1/2+y,1/2-z) phenyl ring, $\mathbf{R^4}$ [C(6)–C(7)–C(8)–C(9)–C(10)–C(15)]. On the other hand, another inter-molecular C–H···π interaction is observed between the hydrogen

atom, H(3A), and the phenyl ring $\mathbf{R^4}$ of different symmetry (1+x,y,z). As a combination of these supramolecular interactions the complex forms a two dimensional network along ab plane (Figure 4).

Complex **2** shows two inter-molecular C–H···π interactions. The hydrogen atom, H(12), attached with C(12), is involved in an inter-molecular C–H···π interaction with a symmetry related (1-x,-1/2+y,1/2-z) phenyl ring, $\mathbf{R^5}$ [C(10)–C(11)–C(12)–C(13)–C(14)–C(15)]. On the other hand, another inter-molecular C–H···π interaction is observed between the hydrogen atom, H(3A), and the phenyl ring $\mathbf{R^5}$ of different symmetry (x,1+y,z). In addition to the C–H···π interactions there is one inter-molecular N–H···π interaction involving the hydrogen atom, H(1A), attached with N(1), and a symmetry related (x,1+y,z) phenyl ring, $\mathbf{R^4}$ [C(6)–C(7)–C(8)–C(9)–C(10)–C(15)]. The complex forms a two dimensional supramolecular network via C–H···π and N–H···π intraction along ab plane (Figure 5). The details of geometric features of both C–H···π and N–H···π interactions are given in Table 4.

*3.2.2 Complex [Cu(L)($\mu_{1,5}$-dca)]$_n$ **(3)***

Complex **3** crystallizes in monoclinic space group *C2/c*. The X-ray crystal structure determination reveals that the copper(II) centres are bridged singly by end-to-end (EE) dca with the formation of a zigzag chain. Perspective view of complex **3** with the selective atom-numbering scheme is shown in Figure 6 and important bond lengths and bond angles are listed in Table 2. The asymmetric unit consists of a copper(II) centre, one deprotonated Schiff base ligand, (L^-), and a dca anion. Each copper(II) centre is coordinated equatorially by one imine nitrogen atom, N(4), one amine nitrogen atom, N(1) and one oxygen atom, O(1), of the tridentate deprotonated Schiff base, $(L)^-$,a nitrogen atom, N(16), of the EE bridged dca ligand. The apical position is occupied by one nitrogen atom N(20)^c (^{c} = x,-1+y,z) of the another EE bridged dca

from a crystallographically related unit to complete elongated square-pyramidal (4 + 1) geometry for each copper(II) center. The Addison parameter (τ) is 0.12, and this confirms the slightly distorted square pyramidal geometry. In the equatorial plane, the Cu–N_{imine} distance [1.940(3) Å] is shorter than the Cu–N_{amine} {2.040(4) Å} distance, as was also observed in complexes **1** and **2**. The deviations of the coordinating atoms N(1), N(4), O(1) and N(16) from the least square mean plane through them are -0.074(3), 0.079(3) -0.077(3) and 0.071(3) Å respectively. As usual for a square pyramid structure, the copper(II) is slightly pulled out of this mean square plane towards the apical donor atom at a distance 0.160(0) Å. The five membered chelate ring Cu(1)–N(1)–C(2)–C(3)–N(4), assumes envelope conformation with puckering parameters Q(2) = 0.448(4) Å and $\phi(2) = 63.7(4)^o$ [45-47]. The shortest Cu···Cu distance in the chain is 7.688(1) Å.

The hydrogen atom, H(1B), attached with N(1) of the Schiff base, is engaged in bifurcated hydrogen bonding interactions with the symmetry related nitrogen atoms, $N(16)^e$ (^{e} = 1-x,y,1/2-z) and $N(20)^f$ (^{f} = 1-x,-1+y,1/2-z), of the bridging dca from an adjacent chain to form a one-dimensional double chains along the crystallographic b axis (Figure 7). The details of hydrogen bonding interactions are given in Table 3. The complex shows two inter-molecular C–H···π interactions. The hydrogen atom, H(8), attached with C(8), is involved in inter-molecular C–H···π interactions with symmetry related (1/2-x,1/2+y,1/2-z) phenyl rings, $\mathbf{R^4}$ [C(10)–C(11)–C(12)–C(13)–C(14)–C(15)] and $\mathbf{R^3}$ [C(6)–C(7)–C(8)–C(9)–C(10)–C(15)]. These two C–H···π interactions constract a zipper structure along b axis (Figure 8). The details of geometric features of the C–H···π interactions are given in Table 4. The complex shows significant π···π stacking interactions between the chelate ring $\mathbf{R^2}$ [Ni–O(1)–C(16)–C(7)–C(6)–N(1)] and symmetry related (1/2-x,1/2-y,-z) aromatic ring $\mathbf{R^4}$ [C(10)–C(11)–C(12)–C(13)–C(14)–C(15)], present in each mononuclear unit with the neighboring units as shown in Figure 8. The π···π stacking

interactions produce a zipper along the b-axis. The detail geometric features of the stacking interactions are given in Table 5.

3.3 Magnetic properties

Variable temperature magnetic susceptibility data over the range 2 – 300 K were collected for powder samples of complexes **1**–**3** (Figures 9 – 11). Each sample exhibited a temperature independent $\chi_M T$ value between 50 – 300 K. Below 50 K, a downturn in the $\chi_M T$ value is observed due to antiferromagnetic exchange coupling between copper(II) ions in these complexes. For example, complex **1** shows a $\chi_M T$ value of 0.804 cm^3 K mol^{-1} at room temperature, which reduces to 0.142 cm^3 K mol^{-1} at 2 K. The plateau value is marginally larger than the spin-only value of 0.75 cm^3 mol^{-1} K (for g = 2.0) expected for two weakly interacting copper(II) ions ($S = {}^1/_2$). Both the $\chi_M T$ vs T and χ_M vs T plots were simulated using the standard Heisenberg-Dirac-van Vleck Hamiltonian, $\hat{H} = -2JS_1 \cdot S_2 + \mu_B gSH$, where all the parameters have their usual meanings. For **1**, the best fit was achieved for g = 2.079 and J = -2.28 cm^{-1} (Figure 9), where the sign of the latter denotes antiferromagnetic coupling between the copper(II) ions. Complex **2**, which like **1** is a discrete dimer, gave a best fit for g = 2.072 but a markedly smaller exchange coupling constant of J = -0.54 cm^{-1} (Figure 10). These are typical values for complexes of this type [48-49]. In both case the fit included a minor contribution stemmed from temperature-independent paramagnetism (TIP) of 169.4 × 10^{-6} cm^3 K mol^{-1} for **1** and 70.7 × 10^{-6} cm^3 K mol^{-1} for **2**. Compound **3** differs from **1** and **2** in that it forms a chain of [Cu(L)($\mu_{1,5}$-dca] units. In this circumstance, the magnetic susceptibility data were modeled using a four copper(II) ions ($S_1 = S_2 = S_3 = S_4 = {}^1/_2$) with equivalent exchange coupling constants ($J_{12} = J_{23} = J_{34}$). The fit shown in Figure 11 yielded g = 2.116 and J = -0.45 cm^{-1} and a TIP contribution of 69.4 × 10^{-6}

cm^3 K mol^{-1}. The values agree well with similar dca bridged polynuclear copper(II) complexes [50-51].

3.4 Magneto-structural correlation

When the end-on pseudo-halide bridge is in basal–basal position, both the experimental values and the theoretical calculations demonstrate that J can be ferromagnetic or ferromagnetic depending mainly on the Cu–N–Cu angle [36]. This reasoning is not valid when the azide bridges are in basal–apical coordination [36]. Therefore the weak interactions among the copper(II) centres in basal–apical azide bridged dinuclear complexes **1** and **2** may be linked with the square pyramidal geometries of copper(II) centres. The magnetic orbital describing the single electron is d_{x2-y2} lying in the basal plane of square pyramidal copper(II) and has only a small contribution on the axis perpendicular to the basal plane and hence no overlap between magnetic orbitals is expected. The variation in the coupling constants of **1** and **2** could thus be linked with the Addison parameters (τ). Lower is the value of τ, less is the deviation from ideal square pyramidal geometry, and lower should be the value of coupling constants. This has been observed in the present case (Table 6). On the other hand, complex **3** features a dca bridged chain. The weak antiferromagnetic coupling (J = -0.45 cm^{-1}) inside the chain is obviously due to the longer distance (7.688(1) Å) between the copper(II) ions as dca acts as a μ-1,5 bridging ligand.

3.5 IR, UV-Vis and fluorescence spectra

Strong and sharp bands at 1623, 1625 and 1626 cm^{-1} due to azomethine (C=N) groups of Schiff base were routinely noticed in the IR spectra of the complexes **1**, **2** and **3** respectively

[52]. Two bands in the IR spectra of all the complexes are observed in the region 3150-3340 cm^{-1} due to the symmetric and asymmetric N–H stretching vibrations [53]. Complex **1** shows an intense absorption band at 2037 cm^{-1} corresponding to the azide ligand [54]. One sharp and strong band at 2207 cm^{-1} in the IR spectrum of complex **2** indicates the presence of the N bonded NCO group [44]. For complex **3**, the bands at 2290, 2235 and 2159 cm^{-1} indicate the presence of dicyanamide [30].

The electronic spectra of **1-3** in acetonitrile solution display d–d absorption bands at 590, 592 and 593 nm, respectively [36]. The UV absorption bands at 382 for **1**, 314 and 393 for **2**, 382 nm for **3** may be assigned to the ligand to metal charge transfer transitions [56]. The complexes exhibit luminescence in acetonitrile medium. The luminescence data are listed in Table 7 (without solvent correction). These are assigned as intra-ligand $^1(\pi\text{-}\pi^*)$ fluorescence [32].

3.6 Powder XRD

The experimental PXRD patterns of the bulk products are in good agreement with the simulated XRD patterns from single-crystal X-ray diffraction, indicating consistency of the bulk sample. The simulated patterns of the complexes are calculated from the single crystal structural data (Cif files) using the CCDC Mercury software. Figure 12 shows the experimental and simulated powder XRD patterns of complex **3 (**for example**).**

4. Concluding Remarks

In the present study, it has been shown that a monocondensed Schiff base of 1,2-diaminoethane and 2-hydroxy-1-naphthaldehyde could be conveniently synthesized as the copper(II) complexes, $[Cu_2(L)_2(\mu_{1,1}\text{-}N_3)_2]$ **(1)**, $[Cu_2(L)_2(\mu_{1,1}\text{-}NCO)_2]$ **(2)** and $[Cu(L)(\mu_{1,5}\text{-}dca)]_n$

(3). X-ray crystal structure determination confirmed the structures of the complexes. The formation of the complexes was explained by an anion directed cation templating effect. Variable temperature magnetic susceptibility measurements showed the presence of antiferromagnetic interaction among the copper(II) centres in the complexes.

Acknowledgments

This work was supported by the DST, India under FAST Track Scheme (Order No. SR/FT/CS-118/2010, dated 15/02/2012). A.B. thanks the UGC, India, for awarding a Junior Research Fellowship.

Appendix A. Supplementary data

CCDC 1001822, 1001824 and 1001823 contain the supplementary crystallographic data for **1, 2** and **3** respectively. These data can be obtained free of charge via http://www.ccdc.cam.ac.uk/conts/retrieving.html or from the Cambridge Crystallographic Data Centre, 12 Union Road, Cambridge CB2 1EZ, UK; fax: (+44) 1223-336-033; or e-mail: deposit@ccdc.cam.ac.uk.

Reference

[1] R. C. Elder, Aust. J. Chem. 31 (1978) 35-45.

[2] P. J. Burke, D. R. McMillin, J. Chem. Soc., Dalton Trans. (1980) 1794-1796.

[3] S. Banerjee, M. G. B. Drew, C. –Z. Lu, J. Tercero, C. Diaz, A. Ghosh, Eur. J. Inorg. Chem. (2005) 2376-2383.

[4] P. Mukherjee, M. G. B. Drew, A. Ghosh, Eur. J. Inorg. Chem. (2008) 3372-3381.

[5] J. -P. Costes, F. Dahan, M. B. F. Fernandez, M. I. F. Garcia, A. M. G. Deibe, J. Sanmartin, Inorg. Chim. Acta 274 (1998) 73-81.

[6] S. Chattopadhyay, M. G. B. Drew, A. Ghosh, Polyhedron 26 (2007) 3513-3522.

[7] C. Biswas, M. G. B. Drew, A. Figuerola, S. Gómez-Coca, E. Ruiz, V. Tangoulis, A. Ghosh, Inorg. Chim. Acta 363 (2010) 846-854.

[8] C. -C. Zhao, Y. -B. Jiang, A. -L. Cui, H. -Z. Kou, Acta Cryst. E63 (2007) m1824-m1825.

[9] F. Z. C. Fellah, J. -P. Costes, L. Vendier, C. Duhayon, S. Ladeira, J. -P. Tuchagues, Eur. J. Inorg. Chem. (2012) 5729-5740.

[10] L. Rigamonti, A. Cinti, A. Forni, A. Pasini, O. Piovesana, Eur. J. Inorg. Chem. (2008) 3633-3647.

[11] S. Mukherjee, P. S. Mujherjee, Chem. Eur. J. 19 (2013) 17064-17074.

[12] L. Yang, S. Zhang, X. Liu, Q. Yang, Q. Wei, G. Xie, S. Chen, CrystEngComm 16 (2014) 4194-4201.

[13] P. K. Bhowmik, S. Chattopadhyay, Inorg. Chem. Commun. 22 (2012) 14–17.

[14] D. Maity, S. Chattopadhyay, A. Ghosh, M. G. B. Drew, G. Mukhopadhyay, Inorg. Chim. Acta 365 (2011) 25-31.

[15] M. Das, K. Harms, S. Chattopadhyay, Dalton Trans. 43 (2014) 5643–5647.

[16] P. Bhowmik, S. Biswas, S. Chattopadhyay, C. Diaz, C. J. Gómez-García, A. Ghosh, Dalton Trans. 43 (2014) 12414-12421.

[17] S. Mukherjee, P. S. Mujherjee, Dalton trans. 42 (2013) 4019-4030.

[18] M. Das, K. Harms, T. K. Mondal, S. Chattopadhyay, Dalton Trans. 43 (2014) 2936-2947.

[19] S. Chattopadhyay, M. G. B. Drew, C. Diaz, A. Ghosh, Dalton Trans. (2007) 2492-2494.

[20] P. Bhowmik, H. P. Nayek, M. Corbella, N. Aliaga-Alcalde, S. Chattopadhyay, Dalton Trans. 40 (2011) 7916-7926.

[21] S. Mukherjee, P. S. Mujherjee, Acc. Chem. Res. 46 (2013) 2556-2566.

[22] P. K. Bhaumik, K. Harms, S. Chattopadhyay, Polyhedron 68 (2014) 346-356.

[23] S. Jana, P. Bhowmik, M. Das, P. P. Jana, K. Harms, S. Chattopadhyay, Polyhedron, 37 (2012) 21–26.

[24] A. D. Jana, A. K. Ghosh, D. Ghoshal, G. Mostafa, N. R. Chaudhuri, CrystEngComm, 9 (2007) 304-312.

[25] S. R. Batten, K. S. Murray, Coord. Chem. Rev. 246 (2003) 103–130.

[26] S. Ghosh, S. Mukherjee, P. Seth, P. S. Mukherjee, A. Ghosh, Dalton Trans. 42 (2013) 13554-13564.

[27] K. Bhar, S. Choubey, P. Mitra, G. Rosair, J. Ribas, B. K. Ghosh, J. Mol. Struct. 988 (2011) 128–135.

[28] A. Ray, G. Pilet, C. J. Gómez-García, S. Mitra, Polyhedron 28 (2009) 511–520.

[29] D. Mal, R. Sen, C. Adhikary, Y. Miyashita, K. –I. Okamoto, A. Bhattacharjee, P. Gütlich, S. Koner, J. Coord. Chem. 61(2008) 3486-3492.

[30] P. K. Bhaumik, K. Harms, S. Chattopadhyay, Inorg. Chim. Acta 405 (2013) 400–409.

[31] X. -Y. Song, W. Li, L. -C. Li, D. -Z. Liao, Z. -H. Jiang, Inorg. Chem. Commun. 10 (2007) 567-570.

[32] M. Das, S. Chattopadhyay, Transition Met. Chem. 38 (2013) 191–197.

[33] A. Ray, S. Banerjee, R. J. Butcher, C. Desplanches, S. Mitra, Polyhedron 27 (2008) 2409-2415.

[34] A. Escuer, M. A. S. Goher, F. A. Mautner, R. Vicente, Inorg. Chem. 39 (2000) 2107-2112.

[35] E. Ruiz, J. Cano, S. Alvarez, P. Alemany, J. Am. Chem. Soc. 120 (1998) 11122-11129.

[36] S. Chattopadhyay, M. S. Roy, M. G. B. Drew, A. Figuerola, C. Diaz, A. Ghosh, Polyhedron 25 (2006) 2241–2253.

[37] G.M. Sheldrick, Acta Cryst. 64A (2008) 112-122.

[38] G.M. Sheldrick, SHELXS-97 and SHELXL-97, Program for Structure Solution, University of Göttingen, Germany, 1997.

[39] G. M. Sheldrick, SADABS, Software for Empirical Absorption Correction, University of Göttingen, Institute fur Anorganische Chemieder Universitat, Gottingen, Germany, 1999–2003.

[40] C. Freiburg, W. Reichert, M. Melchers, B. Engelen, Acta Cryst. B36 (1980) 1209-1211.

[41] Y. -Z. Zhou, R. -J. Chen, S. -J. Tu, D. -D. Hu, Z. Kristallogr. NCS 220 (2005) 511-512.

[42] A.W. Addison, T. Nageswara, J. Reedijk, J. van Rijn, G.C. Verchoor, J. Chem. Soc., Dalton Trans. (1984) 1349-1356.

[43] P. K. Bhaumik, K. Harms, S. Chattopadhyay, Polyhedron 62 (2013) 179-187.

[44] P. K. Bhaumik, K. Harms, S. Chattopadhyay, Polyhedron 67 (2014) 181–190.

[45] D. Cremer, J. A. Pople, J. Am. Chem. Soc. 97 (1975) 1354-1358.

[46] D. Cremer, Acta Crystallogr. Sect. B 40 (1984) 498-500.

[47] J. C. A. Boeyens, J. Cryst. Mol. Struct. 8 (1978) 317-320.

[48] P. Mukherjee, O. Sengupta, M. G.B. Drew, A. Ghosh, Inorg. Chim. Acta 362 (2009) 3285–3291.

[49] S. Naiya, S. Biswas, M. G. B. Drew, C. J. Gómez-García, A. Ghosh, Inorg. Chim. Acta 377 (2011) 26–33.

[50] R. Karmakar, C. Roy Choudhury, D. L. Hughes, G. P.A. Yap, M. S. El Fallah, C. Desplanches, J.-P. Sutter, S. Mitra, Inorg. Chim. Acta 359 (2006) 1184–1192.

[51] S. Sen, S. Mitra, D. L. Hughes, G. Rosair, C. Desplanches, Inorg. Chim. Acta 360 (2007) 4085–4092.

[52] A. Bhattacharyya, P. K. Bhaumik, P. P. Jana, S. Chattopadhyay Polyhedron 78 (2014) 40–45.

[53] M. das, S. Chatterjee, S. Chattopadhyay, Polyhedron 68 (2014) 205–211.

[54] M. Das, S. Chattopadhyay, Polyhedron 50 (2013) 443–451.

[55] P. K. Bhaumik, K. Harms, S. Chattopadhyay, Polyhedron 68 (2014) 346–356.

[56] S. Jana, R. C. Santra, S. Das, S. Chattopadhyay, J. Mol. Struct. 1074 (2014) 703–712.

Table 1: Crystal data and refinement details of complexes **1-3**.

	1	**2**	**3**
Formula	$C_{26}H_{26}Cu_2N_{10}O_2$	$C_{28}H_{26}Cu_2N_6O_4$	$C_{15}H_{13}CuN_5O$
Formula Weight	637.65	637.63	342.84
Crystal Size [mm]	0.17 x 0.18 x 0.39	0.17 x 0.31 x 0.54	0.08 x 0.37 x 0.40
Temperature(K)	100	100	100
Crystal system	Monoclinic	Monoclinic	Monoclinic
Space group	*P2₁/c*	*P2₁/c*	*C2/c*
a(Å)	5.856(1)	11.781(1)	28.057(3)
b(Å)	11.728(1)	6.632(1)	7.688(1)
c(Å)	18.557(1)	15.922(2)	13.058(1)
β(deg)	90.616(3)	95.083(4)	109.292(4)
Z	2	2	8
d_{calc} (g cm^{-3})	1.662	1.709	1.713
μ(mm^{-1})	1.716	1.767	1.652
F(000)	652	652	1400
Total Reflections	8574	8303	6852
Unique Reflections	2903	2813	2475
Observed data [I > 2 σ (I)]	2323	2295	2094
No. of parameters	189	181	199
R(int)	0.036	0.047	0.075
R1, wR2 (all data)	0.0436, 0.0768	0.0498, 0.0863	0.0702, 0.1557
R1, wR2 [I > 2 σ (I)]	0.0299, 0.0709	0.0355, 0.0805	0.0607, 0.1472

Table 2: Selected bond lengths (Å) and bond angles (^{0}) around copper(II) for complexes **1-3**.

Complex	**1**	**2**	**3**
Bond lengths			
Cu(1)-O(1)	1.906(2)	1.931(2)	1.894(3)
Cu(1)-N(1)	2.010(2)	2.030(2)	2.040(4)
Cu(1)-N(4)	1.937(2)	1.932(2)	1.940(3)
Cu(1)-N(16)	2.009(2)	1.951(2)	2.009(3)
Cu(1)-N(16)$^{\Psi}$	2.483(2)	2.528(2)	-
Cu(1)-N(20)$^{\Psi}$	-	-	2.514(3)
Bond angels			
O(1)-Cu(1)-N(1)	173.86(7)	174.94(8)	173.55(13)
O(1)-Cu(1)-N(4)	92.72(7)	91.81(8)	91.29(13)
O(1)-Cu(1)-N(16)	90.41(6)	92.63(8)	89.75(13)
O(1)-Cu(1)-N(16)$^{\Psi}$	87.44(6)	94.30(7)	-
N(1)-Cu(1)-N(4)	85.32(7)	84.26(8)	84.02(14)
N(1)-Cu(1)-N(16)	93.10(7)	91.65(8)	93.77(14)
N(1)-Cu(1)-N(16)$^{\Psi}$	87.45(7)	82.89(7)	-
N(4)-Cu(1)-N(16)	163.51(7)	171.95(8)	166.19(13)
N(4)-Cu(1)-N(16)$^{\Psi}$	104.99(6)	94.96(7)	
N(16)-Cu(1)-N(16)$^{\Psi}$	91.32(6)	91.40(8)	
O(1)-Cu(1)-N(20)$^{\Psi}$	-	-	100.50(12)

N(1)-Cu(1)-N(20)$^{\Psi}$	-	-	84.72(13)
N(4)-Cu(1)-N(20)$^{\Psi}$	-	-	100.09(12)
N(16)-Cu(1)-N(20)$^{\Psi}$	-	-	93.26(13)
Cu(1)-N(16)-Cu(1)$^{\Psi}$	88.68(6)	88.60(8)	-

$^{\Psi}$ = Symmetry transformations: ^{a} = 1-x,1-y,1-z in **1**, ^{b} = -x,-y,1-z in **2** and ^{c} = x,-1+y,z in **3**.

Table 3: Hydrogen bonding geometry of complexes **1-3**.

Complex	D–H···A	D–H(Å)	D···A(Å)	H···A(Å)	∠D–H···A(°)
1	N(1)-H(1A)···O(1)^{a}	0.90(2)	3.107(2)	2.29(2)	150(2)
	N(1)-H(1B)···N(16)^{d}	0.87(3)	3.046(2)	2.28(3)	147(2)
2	N(1)-H(1B)···O(1)^{b}	0.99	3.168(3)	2.25	154
3	N(1)-H(1B)···N(16)^{e}	0.99	3.246(5)	2.57	125
	N(1)-H(1B)···N(20)^{f}	0.99	3.250(5)	2.39	145

Symmetry transformations: ^{a} = 1-x,1-y,1-z, ^{d} = 2-x,1-y,1-z, ^{b} = -x,-y,1-z, ^{e} = 1-x,y,1/2-z, ^{f} = 1-x,-1+y,1/2-z. D = donor; H = hydrogen; A = acceptor.

Table 4: Geometric features (distances in Å and angles in °) of the C–H···π and N–H···π interactions obtained for **1**, **2** and **3**.

Complex	X–H···Cg(Ring)	H···Cg (Å)	C–H···Cg (°)	C···Cg (Å)
1	C(2)–H(2B)···Cg(5)[g]	2.84	134	3.597(2)
	C(3)–H(3A)···Cg(4)[h]	2.80	137	3.588(2)
	C(3)–H(3B)···Cg(4)[g]	2.85	133	3.606(2)
2	C(3)–H(3A)···Cg(5)[i]	2.55	149	3.433(3)
	C(12)–H(12)···Cg(5)[j]	2.82	145	3.644(3)
	N(1)–H(1A)···Cg(4)[i]	2.76	138	3.552(2)
3	C(8)–H(8)···Cg(3)[k]	2.88	128	3.545(4)
	C(8)–H(8)···Cg(4)[k]	2.86	175	3.809(4)

Symmetry transformations: [g] = 1-x,-1/2+y,1/2-z, [h] = 1+x,y,z, [i] = x,1+y,z, [j] =1-x,-1/2+y,1/2-z, [k] = 1/2-x,1/2+y,1/2-z. Cg(5) = Centre of gravity of the ring **R**^{5} [C(10)–C(11)–C(12)–C(13)–C(14)–C(15)] and Cg(4) = Centre of gravity of the ring **R**^{4} [C(6)–C(7)–C(8)–C(9)–C(10)–C(15)] for complex **1**. Cg(5) = Centre of gravity of the ring **R**^{5} [C(10)–C(11)–C(12)–C(13)–C(14)–C(15)] and Cg(4) = Centre of gravity of the ring **R**^{4} [C(6)–C(7)–C(8)–C(9)–C(10)–C(15)] for complex **2**. Cg(4) = Centre of gravity of the ring **R**^{4} [C(10)–C(11)–C(12)–C(13)–C(14)–C(15)] and Cg(3) = Centre of gravity of the ring **R**^{3} [C(6)–C(7)–C(8)–C(9)–C(10)–C(15)] for complex **3**.

Table 5: Geometric features (distances in Å and angles in °) of the π···π stacking interactions obtained for **3**.

Complex	Cg(Ring I)···Cg(Ring J)	Cg···Cg (Å)	α (°)	Cg(I)···Perp (Å)	Cg(J)···Perp (Å)
3	Cg(2)···Cg(4)[1]	3.441(2)	3.01(16)	3.410(1)	3.404(2)

Symmetry transformation: [1] = 1/2-x,1/2-y,-z.

α = Dihedral Angle between ring I and ring J; Cg(I)···Perp = Perpendicular distance of Cg(I) on ring J; Cg(J)···Perp = Perpendicular distance of Cg(J) on ring I. Cg(2) = Centre of gravity of the ring **R²** [Cu(1)–O(1)–C(7)–C(6)–C(5)–N(4)] for complex **3** and Cg(4) = Centre of gravity of the ring **R⁴** [C(10)–C(11)–C(12)–C(13)–C(14)–C(15)]

Table 6: Main structural and magnetic parameters for complexes **1**, **2** and **3**.

Complex	**Cu-Cu (Å)**	**Cu-azide (basal) (Å)**	**Cu-azide (apical) (Å)**	**Cu-N-Cu (º)**	**τ**	**J (cm^{-1})**
1	3.159(1)	2.009(2)	2.483(2)	88.68(6)	0.17	-2.28
2	3.156(1)	1.951(2)	2.528(2)	88.60(8)	0.05	-0.54
3	7.688(1)	2.009(3)	2.514(3)	-	0.12	-0.45

Table 7: Photophysical data for the complexes **1**-**3**.

Complex	Absorption (nm)	Emission (nm)
1	382	433
2	393	446
3	382	434

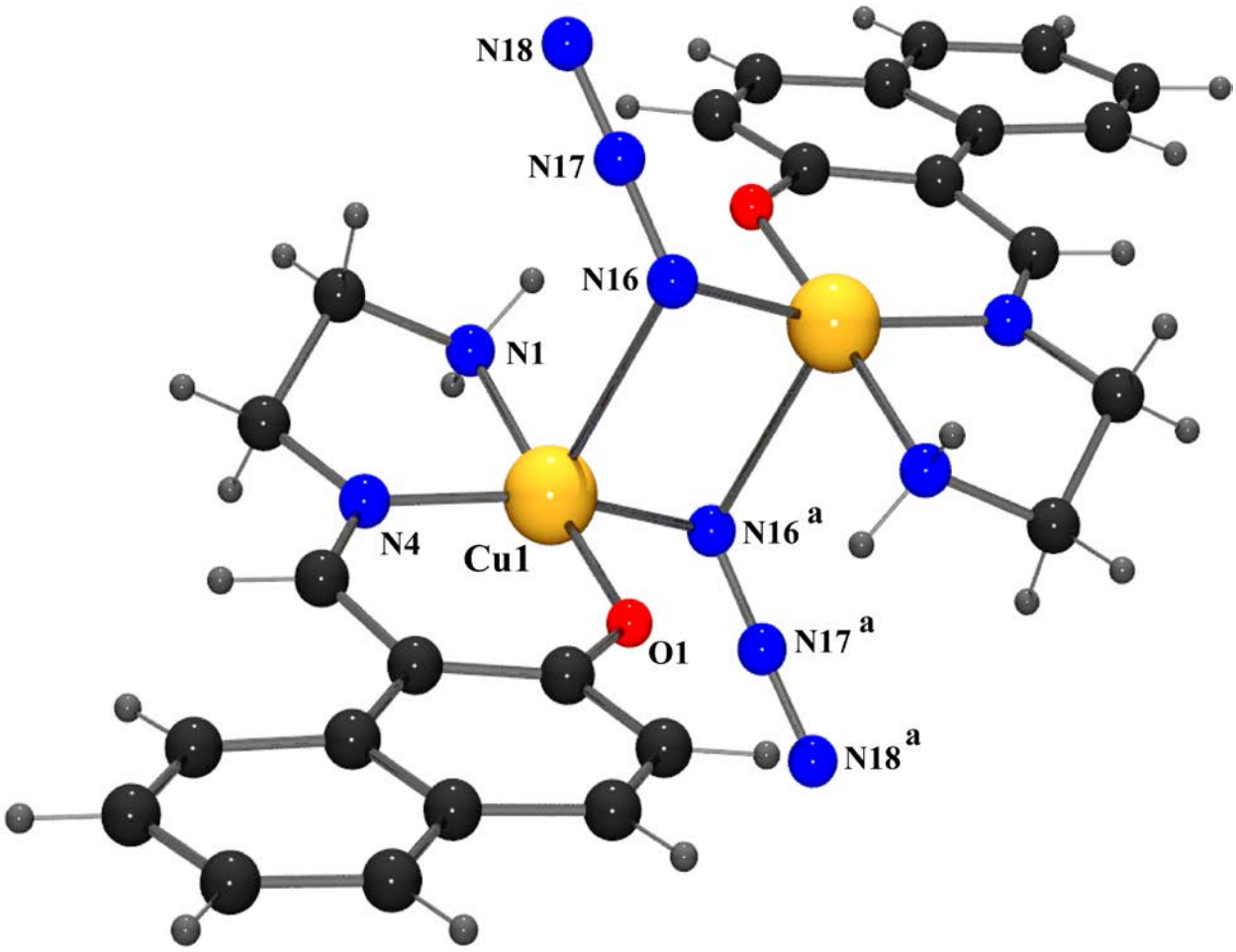

Figure 1: Perspective view of complex **1**. Only the relevant atoms are labeled. Symmetry transformation [a] = 1-x,1-y,1-z.

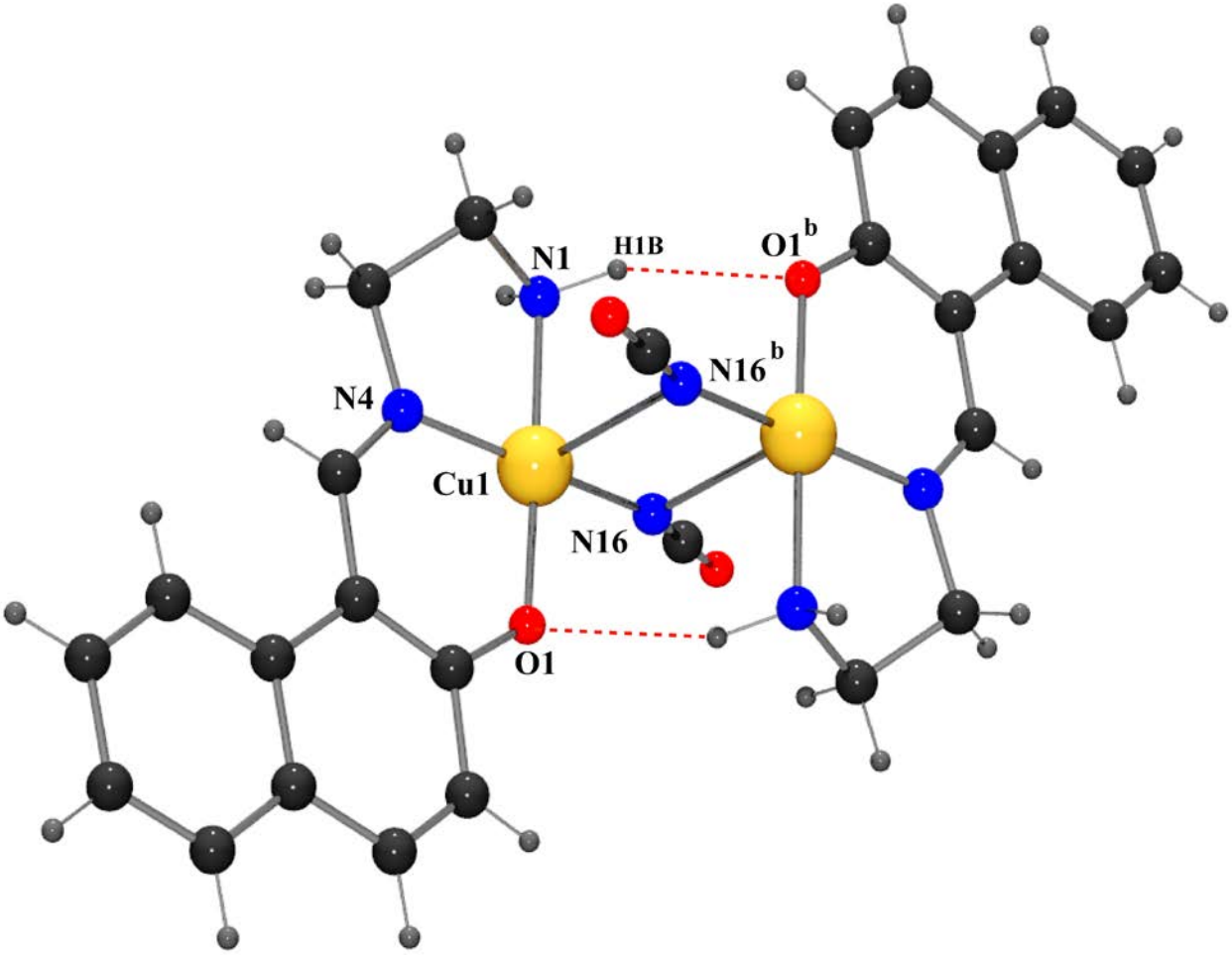

Figure 2: Molecular structure of **2** highlighting the hydrogen bonding interactions with selective atom numbering scheme. Symmetry transformation [b] = -x,-y,1-z.

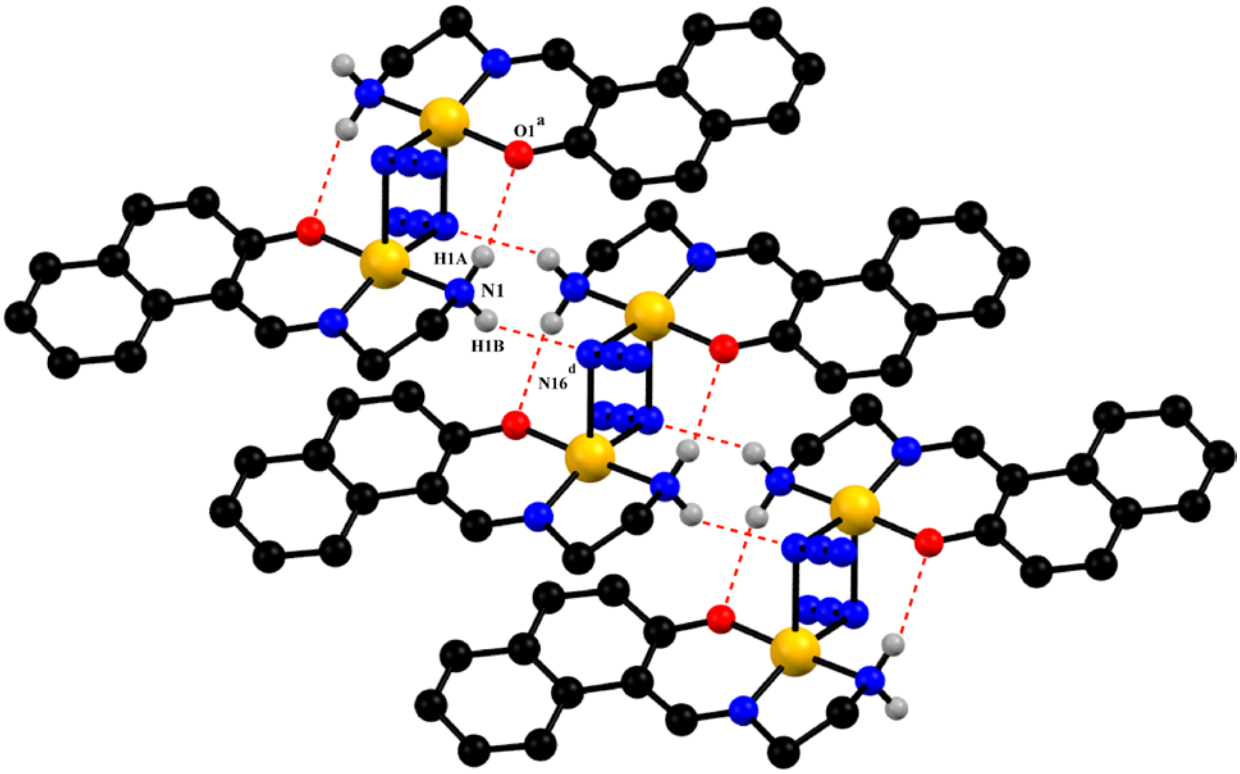

Figure 3: Hydrogen bonded chain of complex **1**. Only relevant hydrogen atoms are shown.

Symmetry transformations [a] = 1-x,1-y,1-z, [d] = 2-x,1-y,1-z.

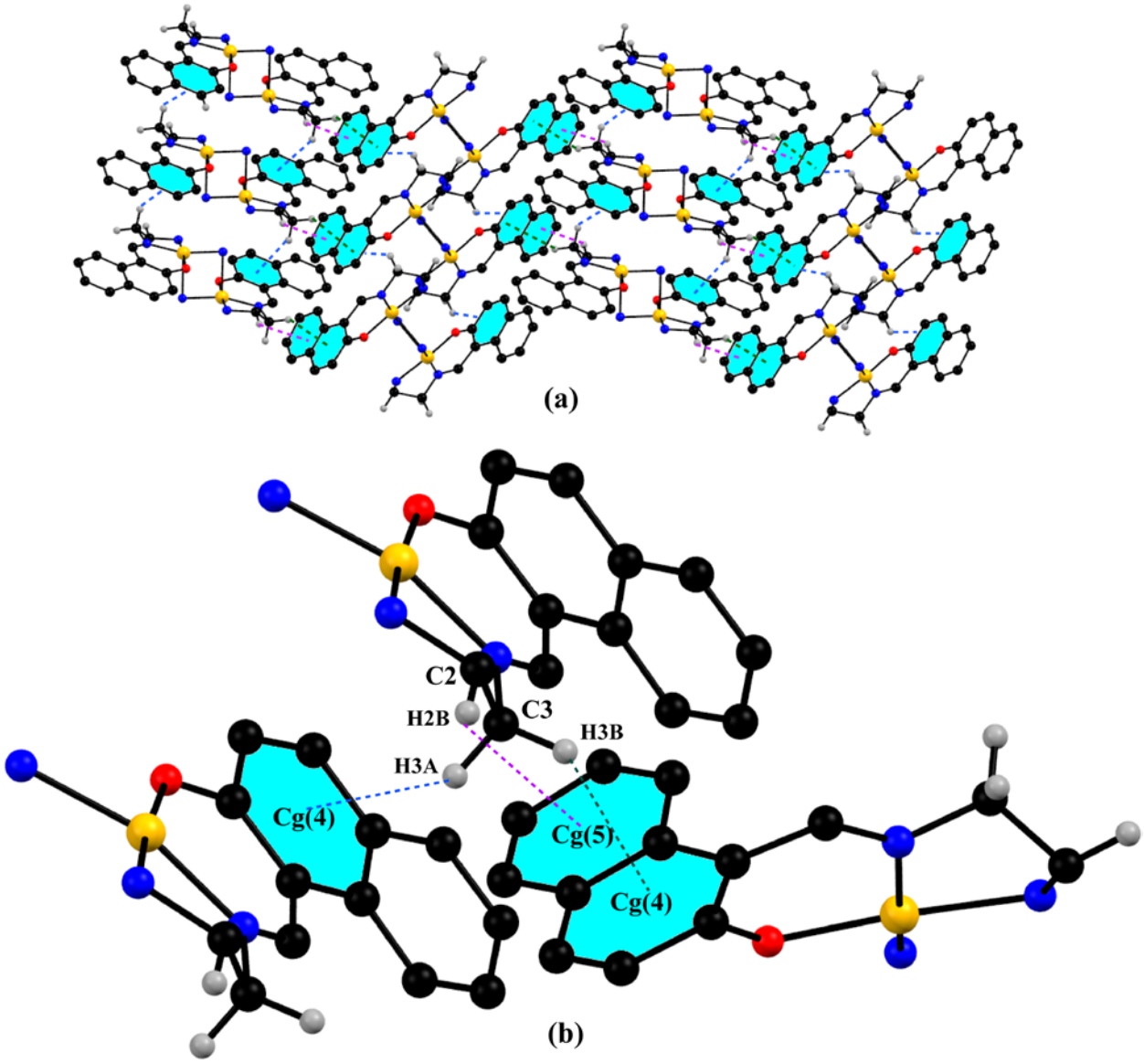

Figure 4: (a) Two-dimensional supramolecular network via C-H···π interactions in complex **1**.

(b) highlighted C-H···π interactions.

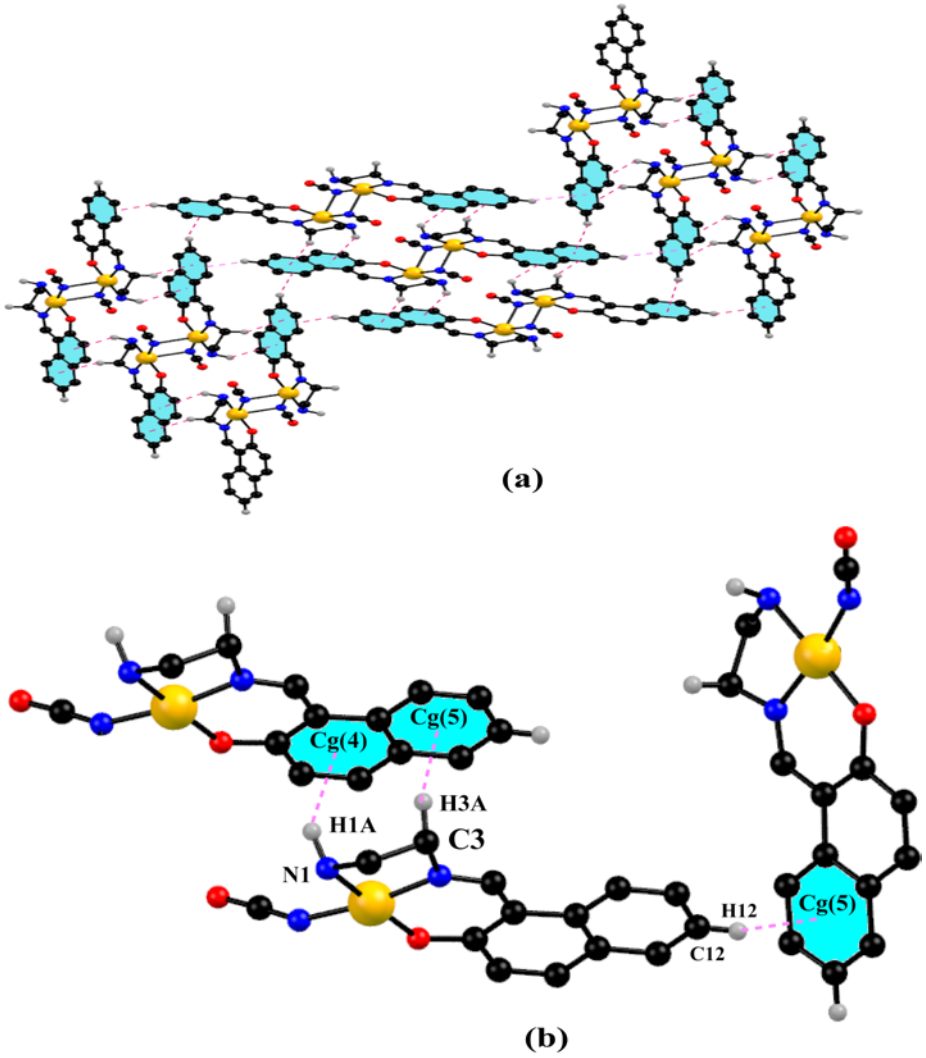

Figure 5: (a) Two- dimensional supramolecular network of complex **2** generated through the C-H···π interactions and (b) highlighted C-H···π interactions. Only relevant hydrogen atoms are shown.

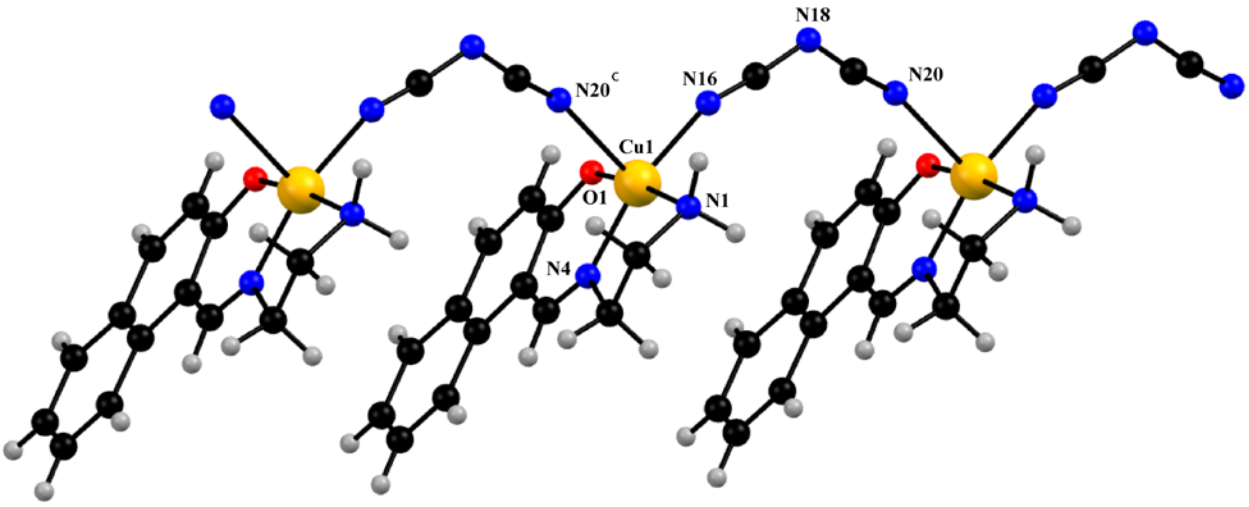

Figure 6: Perspective view of one dimensional chain of complex **3**. Only relevant atoms are labeled. Symmetry transformation ^{c} = x,-1+y,z.

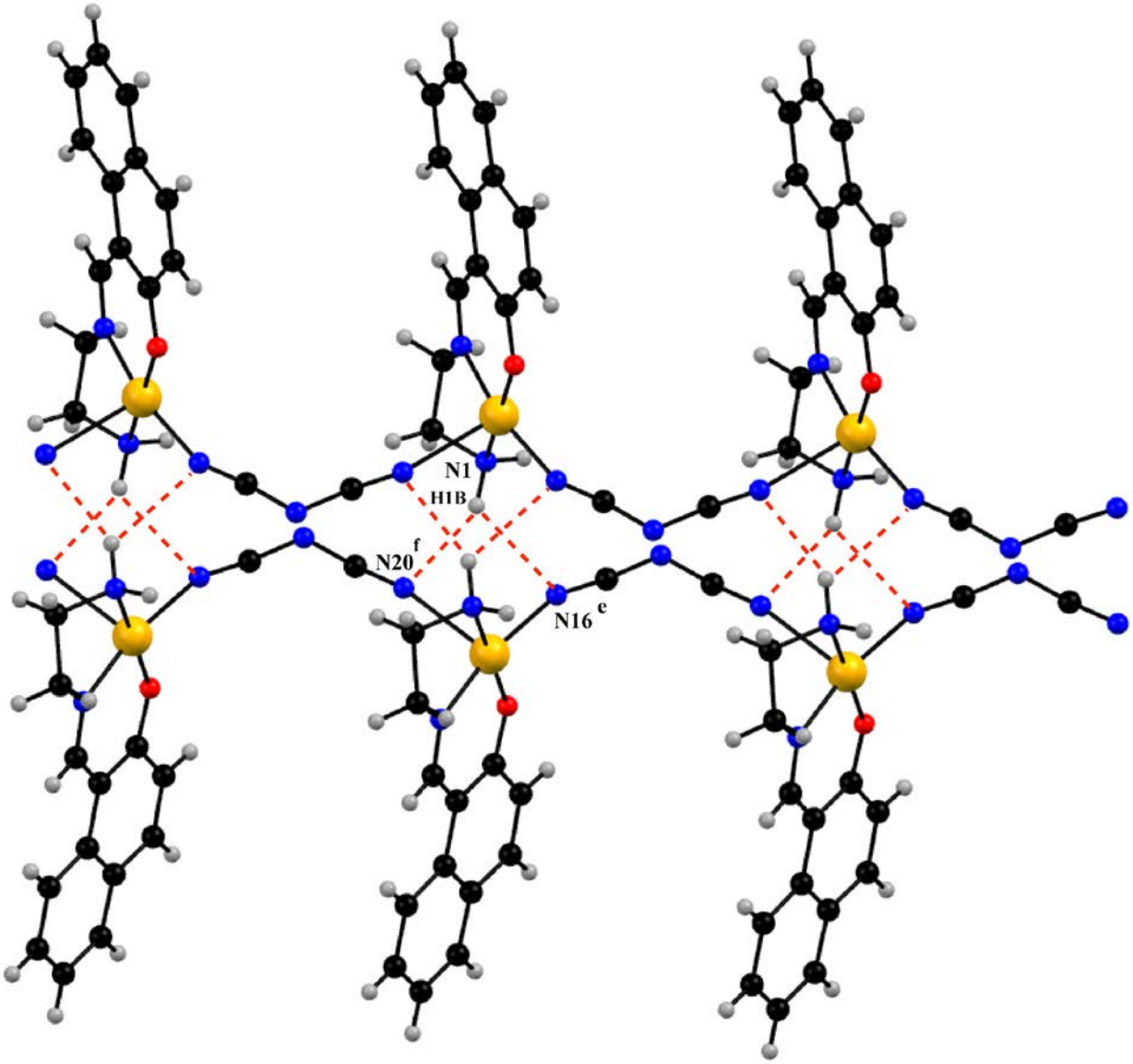

Figure 7: One-dimensional hydrogen bonded double chain structure of complex **3**. Symmetry transformations ^{e} = 1-x,y,1/2-z, ^{f} = 1-x,-1+y,1/2-z.

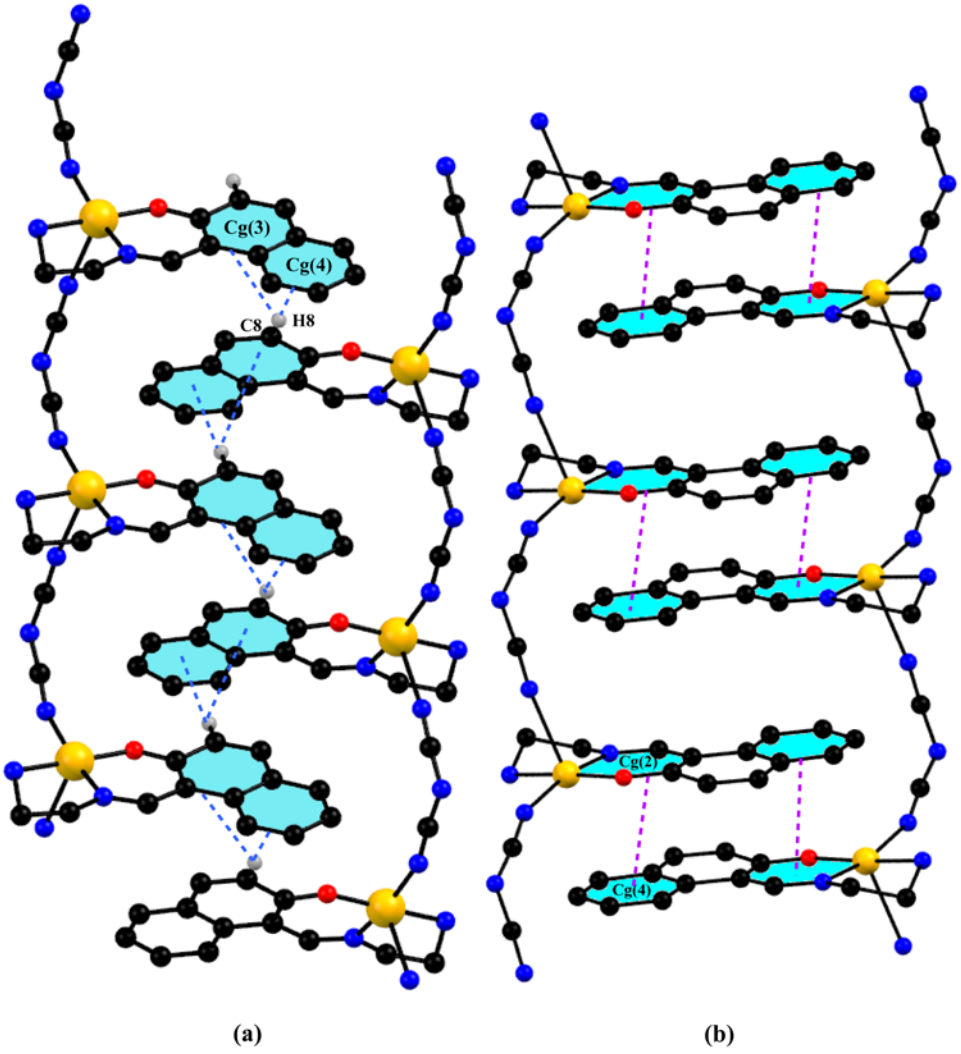

Figure 8: (a) C-H···π interactions and (b) π ···π stacking interactions in complex **3** forming a zipper structure. Only relevant hydrogen atoms are shown.

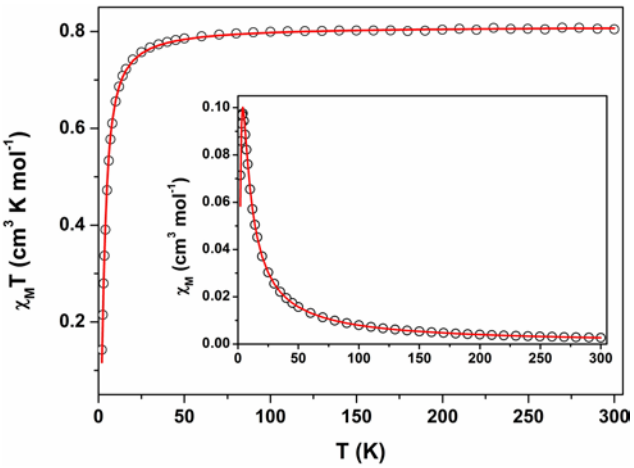

Figure 9: Plot of $\chi_M T$ vs T for a powder sample of **1** in a 1 T external magnetic field. Experimental data shown as open circles and best fit represented by the red line. Inset shows plot of χ_M vs T.

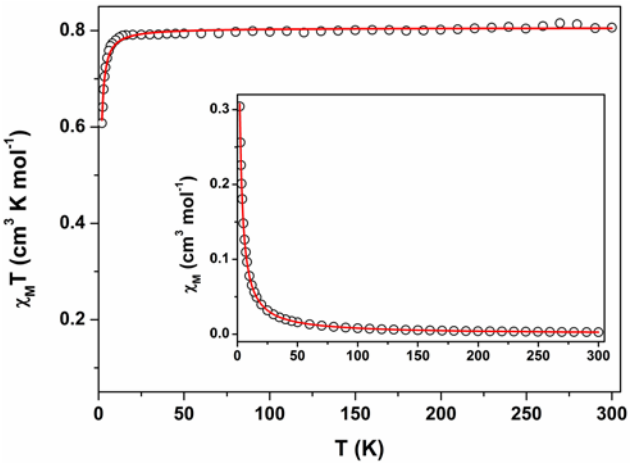

Figure 10: Plot of $\chi_M T$ vs T for a powder sample of **2** in a 1 T external magnetic field. Experimental data shown as open circles and best fit represented by the red line. Inset shows plot of χ_M vs T.

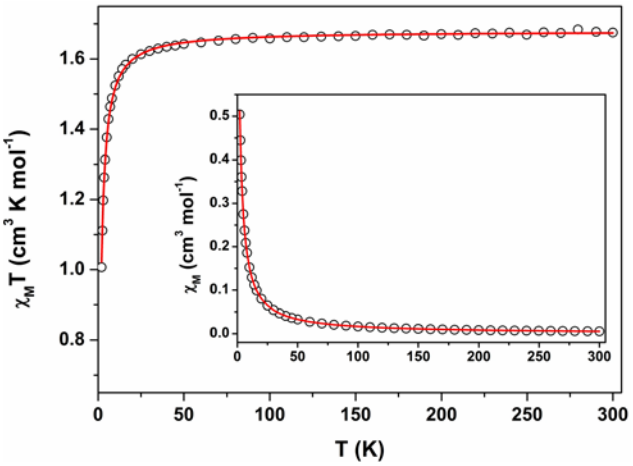

Figure 11: Plot of $\chi_M T$ vs T for a powder sample of **3** in a 1 T external magnetic field. Experimental data shown as open circles and best fit represented by the red line. Inset shows plot of χ_M vs T.

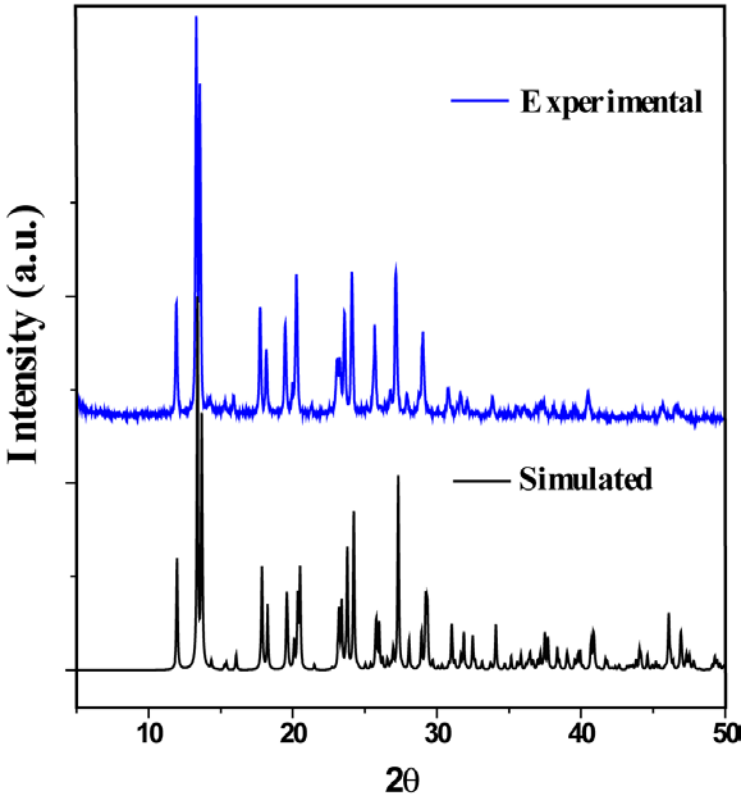

Figure 12: Experimental and simulated PXRD patterns of complex **3** showing the purity of the bulk material.